ONR TECHNICAL REPORT NO. 33

Project N 356-491

Contract: N00014-68-A-0131

A NUMERICAL SIMULATION OF THE CAVITY FILLING PROCESS WITH PVC IN INJECTION MOLDING

by

J. L. Berger and C. G. Gogos

Department of Chemistry and Chemical Engineering
Stevens Institute of Technology
Hoboken, New Jersey 07030

February, 1972

Submitted for publication to
Polymer Engineering and Science

Security Classification

DOCUMENT CONTROL DATA - R & D

Security classification of title, body of abstract and indexing annotation must be entered when the overall report is classified

1. ORIGINATING ACTIVITY (Corporate author)	2a. REPORT SECURITY CLASSIFICATION
Stevens Institute of Technology Hoboken, New Jersey 07030	2b. GROUP

3. REPORT TITLE

A Numerical Simulation of the Cavity Filling Process with PVC in Injection Molding

4. DESCRIPTIVE NOTES (Type of report and, inclusive dates)

Technical Report

5. AUTHOR(S) (First name, middle initial, last name)

James L. Berger and Costas G. Gogos

6. REPORT DATE	7a. TOTAL NO. OF PAGES	7b. NO. OF REFS
February 1972	31	23

8a. CONTRACT OR GRANT NO.	9a. ORIGINATOR'S REPORT NUMBER(S)
N00014-68-A-0131 b. PROJECT NO. NR 356-491	33
c.	9b. OTHER REPORT NO(S) (Any other numbers that may be assigned this report)
d.	

10. DISTRIBUTION STATEMENT

Qualified requesters may obtain copies of this report from the Department of Chemistry and Chemical Engineering, Stevens Institute of Technology, Hoboken, New Jersey 07030

11. SUPPLEMENTARY NOTES	12. SPONSORING MILITARY ACTIVITY
	Chemistry Program, Office of Naval Research, Washington, D.C.

13. ABSTRACT

In this work a numerical simulation of the mold cavity filling process was attempted. The mold filled in this simulation is a disk which hot polymer melt enters through a tubular entrance located at the center of the top plate. The tube is 2.54 cm. long and has a radius of 0.24 cm. The plate separation and outer radius of the disk cavity may be varied. A constant pressure applied at the entrance of the tube causes the flow. The cavity walls are kept at various low temperatures. The reported results are for rigid polyvinyl chloride (PVC).

The general transport equations, i.e. continuity, momentum, and energy, for a constant density power law fluid are used to solve the flow problem. It is assumed that the outer radius of the disk is very much greater than the plate separation, that there is axisymmetry, that only one of the viscous terms in the momentum equation is significant, and that in the flow direction heat conduction is negligible compared with convection. Constant values for the thermal conductivity and heat capacity of the melt are used.

Using the results obtained it is possible to predict "fill times". The formation of a frozen polymer skin as the cavity fills may be followed via the velocity profiles. The temperature profiles which reflect cooling and the amount of viscous heat generated provide the basis for studying resin thermal degradation effects. The pressure and temperature profiles at the instant of fill provide the initial conditions for solving the problems of packing the mold and cooling it under pressure, from which final frozen stains and residual pressures can, in principle, be obtained.

DD FORM 1 NOV 68 1473 (PAGE 1)

S/N 0101-807-6811

Security Classification

A-31408

ABSTRACT

Filling cold mold cavities with hot polymer melts at high pressures is a complicated physical process, which is of great practical interest to the chemical and polymer processing industries. The transport approach to this process of solving the general equations of change with suitable equations of state to describe the flowing material has been largely ignored. No analytic solution is possible, and the non-steady state flow adds a dimension which makes digital computation discouraging because of the core storage and execution time requirements as well as the sophisticated programming required. These considerations have forced the development of mold filling as an empirical art which relies heavily on experience.

In this work a numerical simulation of the mold cavity filling process was attempted. The mold filled in this simulation is a disk which hot polymer melt enters through a tubular entrance located at the center of the top plate. The tube is 2.54 cm. long and has a radius of 0.24 cm. The plate separation and outer radius of the disk cavity may be varied. A constant pressure applied at the entrance of the tube causes the flow. The cavity walls are kept at various low temperatures. The reported results are for rigid polyvinyl chloride (PVC).

The general transport equations, i.e. continuity, momentum, and energy, for a constant density power law fluid are used to solve the flow problem. It is assumed that the outer radius of the disk is very much greater than the plate separation, that there is axisymmetry, that only one of the viscous terms in the momentum equation is significant, and that in the flow direction heat conduction is negligible compared with convection. Constant values for the thermal conductivity and heat capacity of the melt are used.

The resulting differential equations are transformed into difference equations explicitly, except for the energy equation. In this case a Six Point Crank-Nicholson implicit differencing technique was necessary to assure thermal stability of the solution. The difference equations were solved by using a Fourth Order Runge-Kutta integration formula for the velocity profiles and the Thomas method for the temperature profiles. Convergence to the differential solutions is guaranteed but since a lower limit was imposed on the time increment by the core storage limit of the computer facilities (27K) and long execution times, all results are semi-quantitative for the problem as stated.

Using the results obtained it is possible to predict "fill times". The formation of a frozen polymer skin as the cavity fills may be followed via the velocity profiles. The temperature profiles which reflect cooling and the amount of viscous heat generated provide the basis for studying resin thermal degradation effects. The pressure and temperature profiles at the instant of fill provide the initial conditions for solving the problems of packing the mold and cooling it under pressure, from which final frozen stains and residual pressures can, in principle, be obtained.

Finally, because so much of the total pressure drop is dissipated in the entrance tube, and so much viscous heat is generated there, this study indicates that the design of the gate and runner system is perhaps the most important facet of success in mold filling.

INTRODUCTION

For many years studies of injection or transfer molding have dealt with the problem of the mold cavity filling process. Most of these studies have been empirical and experimental, where "moldability" of a given resin is usually related to how far the resin penetrates a mold of a certain shape, such as the spiral mold.[1,2] Another useful empirical criterion used in practice to insure successful molding is that of having a resin viscosity in the range of 10^3 to 2×10^3 poises at 10^3 sec^{-1} at the molding temperature. Of course, the polymer resin has to be thermally stable at that temperature.

As the industry turned to molding parts having more complex geometries, larger surface areas and thinner crosssections, more reliable criteria had to be developed. Thus, recently experimental molds, instrumented with pressure gauges and thermocouples at various positions have been constructed.[3,4] No experimental results, which adequately measure the pressures and temperatures developed in the mold as it is filling, have been reported as yet. Furthermore, and perhaps this is more significant, several people have made an attempt to treat the mold filling process as a problem of combined transport of momentum and energy.[3,5] That is, a "transport phenomena" approach has been applied to this transient and nonisothermal flow problem. The resulting system of coupled partial differential equations cannot be solved analytically. By making liberal use of certain physical assumptions to simplify the mathematical problem, a difference approximation to the solution may be obtained using numerical techniques and a digital computer.

Pearson in his book "Mechanical Principles of Polymer Melt Processing" has outlined a numerical method for solving the problem.[5] The mold is a geometrically simple flat circular cavity of uniform shallow depth h with an

entry point at the center. In deriving the flow and energy equations he assumes

1. Constant resin density ρ
2. Velocity vector is given by $[u(r,x,t), o, o]$
3. Lubrication approximation; $\frac{\partial u}{\partial r} << \frac{\partial u}{\partial x}$
4. Axisymmetry (no θ dependence) and symmetry about the plane $x = 0$
5. Compared with the viscous term, the acceleration, inertia and gravitational terms in the momentum equation are negligible
6. Heat conduction is negligible in the flow direction compared with convection.
7. Viscous energy dissipation (VED) term, $\tau_{rr} \frac{\partial u}{\partial r}$ is negligible compared with $\tau_{rx} \frac{\partial u}{\partial x}$.

Furthermore, he imposes the following boundary conditions:

a. no slip at the wall
b. there is a steady supply of melt at constant temperature T_1 enetering the cavity
c. the heat transfer coefficient L at the walls, which are held at T_o, is constant and defined by

$$\pm k \left(\frac{\partial T}{\partial x}\right)_{x = \pm h/2} = L\left[T_o - T(r, \pm h/2, t)\right] \qquad (1)$$

d. the melt occupies the region $r \leq R$ so that the moving front $R(t)$ is given by

$$R^2 = a^2 + \frac{1}{\pi h} \int_0^t Q(\tau)d\tau \qquad (2)$$

Using this equation to determine front position $R(t)$ ignores the fact that the front actually has a velocity profile. However, this is not a serious drawback so long as $Q(t)$ is accurately described.

e. The average temperature of the newly formed front is given by

$$T\left[R(t+\Delta t), x, t+\Delta t\right] = \int_{-h/2}^{h/2} \frac{u[R(t),x]\, T[R(t),x]}{Q/2\pi R(t)}\, dx \qquad (3)$$

The above equation has no physical significance. Averaging over quantities based on averages of known quantities does not provide accurate information to predict unknowns. Certainly x should not appear on the left-hand side.

The injection system is further described by Pearson as being characterized by a uniform flow rate in the early part of the cycle followed by a uniform pressure drop, $\int_a^R \frac{\partial p}{\partial r}\, dr = -P$, once the pressure drop reaches P. This description is unsatisfactory when the effects of the runners and gate are considered.

He then suggests a numerical method for solving the problem as he described it for a power law fluid. We attempted to program his model, but found certain inconsistencies in the description and numerical edition scheme.

It is not surprising from previous comments that no meaningful average temperature for the newly formed front was obtained using equation 3. The integral on the right-hand side of this equation is totally insensitive to the relative position of the newly formed front to that of the previous front. Since all the function values are representative of an existing situation and Δt does not appear either implicitly or explicitly, the predicted average temperature is always T_1. Several variations of equation 3 which introduced time implicitly also failed. We calculated the detailed temperature profile

of the front using a heat balance in that region, and used the cup average temperature to calculate the average temperature. We tried the explicit differencing technique that Pearson suggested be used for the energy equation and found that it becomes unstable because of errors associated with this approximation. After a certain point the predicted temperatures were either unreasonably high or even negative.

Barrie[6] describes a method for estimating the pressure developed at the entry point of a similar disk mold as a function of flow rate. For a power law fluid under isothermal conditions, the integrated momentum equation establishes that the pressure necessary to support radial disk flow has two components.[7] One arises from the shear stresses

$$(P_s)_o = \frac{2m}{h^{1+2n}} \left(\frac{6Q}{2\pi}\right)^n \frac{1}{1-n} \left[R^{1-n} - a^{1-n}\right] \tag{4}$$

and the second is due to the hoop stresses

$$(P_H)_o = \frac{2Q}{4\pi h}\left[\frac{1}{a^2} - \frac{1}{R^2}\right] \tag{5}$$

Hoop stresses, $T_{\theta\theta}$, cannot be ignored at high shear rates ($10^3 \leq \dot{\gamma} \leq 10^5 sec^{-1}$).

However, in the nonisothermal situation a layer of frozen polymer appears in time which reduces the effective plate separation. Its thickness Δx can be approximately estimated assuming an infinite slab of melt at T_1 is in contact with a thermally conducting wall at T_o, provided that the "freeze off" (i.e., T_g or T_m) temperature and thermal diffusivity[8] are known. Alternatively he proposes a purely empirical expression to estimate Δx. Substituting the reduced separation into the expressions for the pressure components and adding them yields the pressure estimate.

Since the detailed flow behavior was ignored, it is not surprising that good agreement with the observed pressures is obtained only when the empirical estimate of Δx is used. Our results predict a layer of frozen polymer which increases in thickness as one follows it away from the disk entrance at any time. At the instant of fill the difference in pressure at the disk entrance for the isothermal and nonisothermal flows was only about 4 1/2%. We can, therefore, confirm that such a slight modification of the isothermal momentum equations should result in good pressure estimates. Furthermore, at high flow rates the time required to fill the cavity will be unaffected by the wall temperature, making the isothermally predicted fill times reasonably. The implicit steady state assumption used in Barrie's work is the most misleading, since it implies that the entrance pressure has a unique value when the cavity is being filled at a constant flow rate. This is true at any instant but both change with time. To say that the cold cavity is being filled at a constant flow rate during which time the pressure at the disk entrance is also constant, is inconsistent, since more pressure is required to keep a colder material flowing at a given rate than a hotter one.

Harry and Parrot[3] are, to our knowledge, the first investigators to propose and execute a numerical solution to the problem of a hot melt flowing into a cold empty cavity. Choosing a co-ordinate system that moves along with the polymer front, they simulate the filling of rectangular slits with polystyrene at 11,660 psi. The average velocity, position, temperature and velocity profiles of the melt front are reported at various times during the filling process. The simplifying assumptions made in obtaining the coupled equations of momentum and energy are:

1. The pressure gradient in the flow direction is constant at any given instant i.e., $\left.\frac{\partial P}{\partial Z}\right|_t \neq f(Z)$
2. The effect of cavity edges is neglected.
3. The fluid is incompressible.
4. Conductivity, density and heat capacity are constant.
5. Mold surface temperature is constant.
6. Flow is one dimensional.

The effect of the runners and the gate are neglected in the simulation. They have attempted to account for the two controls, pressure and flow rate, of the injection molding machine. Initially flow may be roughly equal to the maximum output rate of the pump, since the hot melt does not offer sufficient resistance to obtain the preset source pressure. When sufficient resistance is experienced, it is the maximum source pressure that controls the injection mold filling operation. The time increment used computationally is not preset but determined by the temperature changes, a considerable advantage. The ability of the simulation to predict short shots and successful fills was experimentally verified. However, the observed and predicted short shot lengths or fill times were different. This is a worthwhile piece of work. Perhaps the most serious assumption is that of a constant pressure gradient.

Finally, it is worth mentioning a work which concerns itself with the cooling of a molding part after the cavity has been filled. The unsteady state heat conduction equation for a cylindrical mold filled with polyethylene and cooling under pressure was solved numerically by Kenig and Kamal.[4] Their rigorous analysis accounted for the temperature dependence of density, specific heat and thermal conductivity. The equation of state used to describe the melt behavior is

$$(P + \pi) \cdot (V - \omega) = R'T \,, \qquad (6)$$

The predicted temperature profiles matched those measured by the instrumented mold within ± 5°F except at short times in the region near the cold wall. What mostly interested us was the statement that, when constant properties were assumed, the numerical temperature stability depended on the choice of these values and the space and time increments employed in the numerical solution. We also observed that the choice of Δt did affect thermal stability and we did use constant density, specific heat and thermal conductivity.

DESCRIPTION OF THE PROBLEM

The following are the essential features of the problem that we attempted to solve numerically: A disk-shaped cavity, shown in Fig. 1, the walls of which are kept at a temperature T_o, is being filled with a non-Newtonian polymer melt which enters the cavity at a constant temperature T_1 through a tube at the center of one of the cavity plates. The polymer melt is forced into the cavity through a constant pressure (PRES) at the tube entrance. Pressure drops, which for a fixed position are time dependent, occur both along the tube axis and the disk radial position. The pressure gradients are not assumed to be linear but are calculated.[9]

We assume throughout this work that the melt density is not a function of temperature or pressure. This is a serious physical assumption, but it seems to have a small effect on the velocity and temperature fields in nonisothermal polymer melt flows.[10] The constant density assumption dictates that the volumetric flow rate is a function of time only.

The following two equations hold for the physical situations considered in this work

$$QTUBE = \frac{n\pi a^3}{3n+1}\left(\frac{a\ DPTUBE}{2mL}\right)^{1/n} \qquad (7)$$

Where: n = flow index of the power law equation

m = consistency index of the power law equation

DPTUBE = total pressure drop across the tube

QTUBE = volumetric flow rate across any tube cross-section

Equation (7) is simply Poiseuille's equation for a power law or Newtonian fluid (n = 1).

It is also always true for all the cases under consideration that

$$PRES = PLEVEL(t) + DPTUBE(t) \tag{8}$$

Where: PLEVEL = the hydrostatic pressure level at the cylindrical surface r = a .

The transport equations needed to solve the flow and heat transfer problem involved in the cavity filling process are the continuity, r-component momentum and thermal energy. The flow is laminar; $u = v_r = u(r,x,t)$ and $v_\theta = v_x = 0$. There are no gravitational forces in the radial direction and the acceleration term is neglected in the r-momentum equation. We also further assume that u/r and $\partial u/\partial r \ll \partial u/\partial x$, This is a good assumption for cases where the melt front has advanced to large radial positions, but relatively poor for very short times in the cavity filling process. It is worth mentioning at this point that, since in our solution method we make use of the lubrication approximation technique, the obtained velocity field will be, as stated above, a function of the radial position. The assumption $\partial u/\partial r \ll \partial u/\partial x$ is used only to eliminate a stress component in the momentum equation. Thus, the continuity and momentum equations become:

$$\rho/r \frac{\partial}{\partial r}(ru) = 0 \tag{9}$$

$$\frac{\partial p}{\partial r} = -\frac{\partial \tau_{rx}}{\partial x} \tag{10}$$

The Power Law constitutive equation for the flowing melt is

$$\tau_{rx} = -2m\left|\frac{\partial u}{\partial x}\right|^{n-1}\frac{\partial u}{\partial x} \tag{11}$$

Where: n - flow index

m - consistency index; $m = A\exp(\Delta E/RT)$ (12)

Combining equations 10 and 11

$$\frac{\partial p}{\partial r} = -\frac{\partial}{\partial x}\left[-m\left|\frac{\partial u}{\partial x}\right|^{n-1}\cdot\frac{\partial u}{\partial x}\right] \tag{13}$$

Thus, if $\partial p/\partial r \neq f(x)$, integrating the above

$$\frac{\partial p}{\partial r} = \frac{m}{x}\left|\frac{\partial u}{\partial x}\right|^{n-1}\frac{\partial u}{\partial x} \tag{14}$$

In Region 1, $0 \leq x \leq h/2$ (See Figure 1)

$$x > 0\ ,\quad \partial p/\partial r < 0\ ,\ \text{and}\ \frac{\partial u}{\partial x} < 0$$

Thus, $$\left|\frac{\partial p}{\partial r}\right| = \frac{m}{x}\left[-\frac{\partial u}{\partial x}\right]^n \tag{15}$$

Therefore,

$$u(x,r,t) = -\left[-\frac{\partial p}{\partial r}\right]^S \int_{h/2}^{x}\left(\frac{x}{m}\right)^S dx \tag{16}$$

where: $S = 1/n$

The volumetric flow rate, assuming symmetry about $x = 0$, is:

$$Q(t) = 4\pi r \left[-\frac{\partial p}{\partial r} \right]^S \int_0^{h/2} \frac{x^{S+1}}{m^S} dx \qquad (17)$$

or

$$\left| \frac{\partial p}{\partial r} \right| = \left[\frac{Q(t)}{4\pi r \int_0^{h/2} \frac{x^{S+1}}{m^S} dx} \right]^{1/S} \qquad (18)$$

Equation 18 is used to calculate $(\partial p/\partial r)$.

Integration of 18 with boundary condition $p(r_{ik}, t) = 0$, r_{ik} is the position of the melt front, leads to

$$p(r,t) = \left[\frac{Q(t)}{4\pi \int_0^{h/2} \frac{x^{S+1}}{m^S} dx} \right]^n \cdot \frac{r_{ik}^{1-n} - r^{1-n}}{1-n} \qquad (19)$$

Evaluated at the entrance $(r = a)$

$$p(a,t) = \text{PLEVEL} = \left[\frac{\text{QTUBE}}{4\pi \int_0^{h/2} \frac{x^{S+1}}{m^S} dx} \right]^n \cdot \frac{r_1^{1-n} - a^{1-n}}{1-n} \qquad (20)$$

The above equations are coupled, through $m = m(T)$, with the thermal energy balance, which for incompressible fluids is[11]

$$\rho C_p \frac{DT}{Dt} = -(\vec{\nabla} \cdot \vec{q}) - (\underset{\sim}{\tau} : \underset{\sim}{\nabla} v) \qquad (21)$$

Where: $\frac{D}{Dt}$ --- Substantial derivative

$\vec{q} = -K\vec{\nabla}T$ the thermal energy flux

For the flow assumed and further assuming that the thermal conductivity, K, is constant and that heat conduction in the radial direction, $(K/r)\frac{\partial}{\partial r}(r.\partial T/\partial r)$, is negligible, equation 21 becomes

$$\rho C_p\left(\frac{\partial T}{\partial t} + u\frac{\partial T}{\partial r}\right) = K\frac{\partial^2 T}{\partial x^2} - \tau_{\theta\theta}\frac{u}{r} - \tau_{rx}\frac{\partial u}{\partial x} \qquad (22)$$

Note that in the above equation the hoop stress $\tau_{\theta\theta}$ is not neglected, while it is neglected in the momentum equation. The Power Law constitution equation has to be modified because of the inclusion of the term $\Delta_{\theta\theta} = 2\frac{u}{r}$.

Thus $\tau_{\theta\theta} = -m\left(\underset{\sim}{\Delta} : \underset{\sim}{\Delta}/2\right)^{(n-1)/2} \cdot \frac{u}{r}$ becomes

$$\tau_{\theta\theta} = -m\left(\frac{u}{r}\right)\left[2\left(\frac{u}{r}\right)^2 + \left(\frac{\partial u}{\partial x}\right)^2\right]^{(n-1)/2}$$

and

$$\tau_{rx} = -m\left(\frac{\partial u}{\partial x}\right)\left[2\left(\frac{u}{r}\right)^2 + \left(\frac{\partial u}{\partial x}\right)^2\right]^{(n-1)/2}$$

Thus the energy balance, equation 22, becomes

$$\rho C_p\left(u\frac{\partial T}{\partial r} + \frac{\partial T}{\partial t}\right) = K\frac{\partial^2 T}{\partial x^2} + \eta\left[\left(\frac{\partial u}{\partial x}\right)^2 + \left(\frac{u}{r}\right)^2\right] \qquad (23)$$

where

$$\eta = 2m(T)\left|2\left(\frac{u}{r}\right)^2 + \left(\frac{\partial u}{\partial x}\right)^2\right|^{(n-1)/2} \qquad (24)$$

The following boundary and initial conditions are used:

$$K\left(\frac{\partial T}{\partial x}\right)_{x=\pm h/2} = L[T_o - T(r, \pm h/2, t)] \qquad (25)$$

where L: constant heat transfer coefficient

$$T(r = a,x,t) = T_1 \tag{26}$$

$$T(r,x,t = 0) = T_1 \tag{27}$$

The temperature of the newly created front $T(r_{ik},x,t)$ is found by adjusting the temperature of the previous front predicted by the energy equation at the new time $T(r_{ik-1},x,t)$ to account for heat generated by VED as well as heat lost to the walls and empty cavity downstream during the past computational time increment. For the heat transfer to the empty cavity forced convection is assumed with $h = 50$ Kcal/m^{2}hr^{o}C.[11] The heat transfer coefficient L is estimated by dividing the thermal conductivity of strainless steel by a typical cavity wall thickness, about 1 inch. The value of L used is of the order of 500 Kcal/m^{2}hr^{o}C.

NUMERICAL CALCULATING SCHEME

A numerical simulation of the flow problem described is achieved by replacing all the necessary differential and integral equations by their finite difference forms.[12] Rather than represent the flowing system in terms of continuous functions of space and time, $u(r,x,t)$, $T(r,x,t)$, $p(r,t)$ etc., one uses their values $u_{i,j,k}$; $T_{i,j,k}$; $p_{i,k}$ at a discrete number of spatial points and times given by the indices i,j,k .

$$r_i = r_{i-1} + \Delta r_i \qquad x_j = j\Delta x \qquad t_k = k\Delta t$$

and $$r_1 = a \quad , \quad h = ?(L-1)\Delta x \qquad 0 \leq j \leq L$$

Thus, $u_{i,j,k} = u(r_i, j\Delta x , k\Delta t)$.

The positions r_i are determined by the initial condition that the mold be empty at $t = 0$ and the boundary condition that if the moving front is designated r_{ik}, that the melt occupies the region $r \leq r_{ik}$. Integrating the continuity equation subject to these constraints we obtain for constant volumetric flow rate Q

$$r_{ik}^2 = r_{ik-1}^2 + \frac{Q \cdot \Delta t}{\pi h} \tag{28}$$

So the positions r_i are merely previous locations of the moving polymer melt front.

Since the melt is cooling as it advances into the cavity, one must account for the fact that the polymer will freeze, i.e., solidify, when it reaches a certain temperature. Because of the cold cavity walls the cessation of flow will start there and gradually move inward toward the center of the flow region. This frozen material near the walls prevents further flow in this region. Consequently, the hot polymer finds the cavity becoming narrower as cooling progresses. The spacing h in the continuity equation is thus replaced by h_e. All the material in the region $h_e \leq x < h$ is frozen whereas, if $0 \leq x < h_e$ the material is flowing. The position of the new front is now given by

$$r_{ik}^2 = r_{ik-1}^2 + \frac{Q \cdot \Delta t}{\pi h_e} \tag{29}$$

The equation of motion for a power law fluid, equation 18, is numerically represented in the following manner. The left-hand side, DPDR(I,K), is evaluated for each radial position and time by using the finite difference form of equation 18. Therefore, the pressure gradient is not assumed constant. Simpson's rule is used to approximate the integral.[13]

The local fluid velocity at each height, (J) position, is obtained by beginning at the wall (where it is always zero because of the no slip boundary condition) and calculated toward the centerline using DPDR(I,K) and the Fourth Order Runge-Kutta scheme[14] to calculate the unknown quantity DELV, shown schematically below.

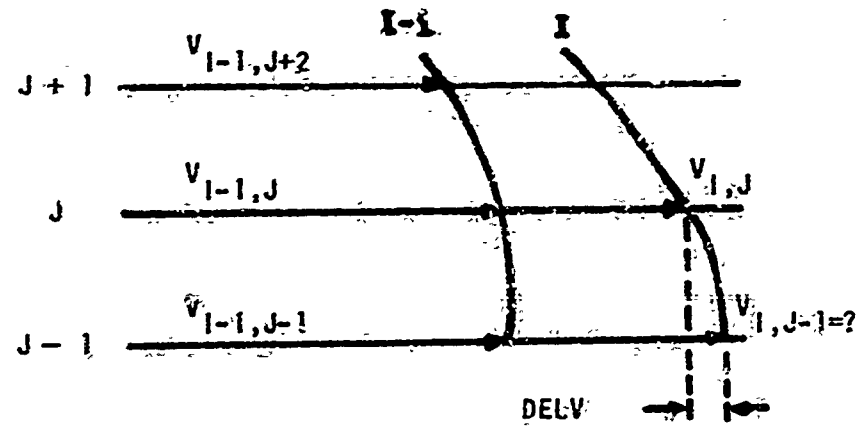

To determine whether DPDR(I,K) is correct, the pressure at the entrance of the disk, PLEVEL, must also be computed from DPDR(I,K). If PLEVEL (equation 20) added to the pressure drop through the tube DPTUBE equals the total pressure drop PRES, then the equation of motion is satisfied. If not, QTUBE on the right-hand side of equation 18 is appropriately varied until equation 8 holds.

The energy equation, 23 and 24, is a parabolic, non-homogeneous partial differential equation. It is transformed by the Crank-Nickolson "six point implicit form" method[16] to a system of (L-1) simultaneous equations,

$$T_{i,j+1,k+1} - 2\left(1 + \frac{1}{\xi}\right)T_{i,j,l+1} + T_{i,j-1,k+1} + T_{i,j,k} - 2\left(1 - \frac{1}{\xi}\right)$$

$$T_{j,j,k} + T_{i,j-1,k} = \Delta t \left\{\left[\frac{u(T_{i,j,k} - T_{i-1,j,k})}{r_i - r_{i-1}}\right] - \left[\frac{n}{\rho C_p}\left(\frac{\partial u}{\partial x}\right)^2\right] -$$

$$\left[\frac{2n}{\rho C_p}\left(\frac{u}{r}\right)^2\left\{2\left(\frac{u}{r}\right)^2 + \left(\frac{\partial u}{\partial x}\right)^2\left\{\frac{n-1}{2}\right]\right\}\right\} \qquad (30)$$

where $\xi = k\Delta t/\rho C_p(\Delta x)^2$ is a dimensionless group.

Each equation is rearranged with the unknown quantities on the left and cast in the matrix form:

$$\begin{bmatrix} A_1 & B_1 & \cdots & & \\ C_2 & A_2 & B_2 & \cdots & \\ & C_3 & A_3 & B_3 & \cdots \\ & \cdots & C_{L-2} & A_{L-2} & B_{L-2} \\ & & & C_{L-1} & a_{L-1} \end{bmatrix} \cdot \begin{bmatrix} T_{i,1,k+1} \\ T_{i,2,k+1} \\ " \\ " \\ T_{i,L-1,k+1} \end{bmatrix} = \begin{bmatrix} D_1 \\ D_2 \\ " \\ " \\ D_{L1} \end{bmatrix} \qquad (31)$$

The above system of equations, which now represents the energy balance in difference form, is solved by the method of Thomas.[18] Details of the solution as well as copies of the computer program may be obtained through the authors. Conduction in the flow direction is

$$\frac{k}{r}\frac{\partial}{\partial r}\left(r\frac{\partial T}{\partial r}\right) = \frac{k}{r}\left(\frac{\partial T}{\partial r} + \frac{\partial^2 T}{\partial r^2}\right) + k\frac{\partial^2 T}{\partial r^2} \qquad (32)$$

In difference form

$$q_d = \frac{THCOH}{[R(I) + R(I-1)]/2} * \frac{T(I,J,K) - T(I-1,J,K)}{R(I) - R(I-1)} +$$

$$THCON * \frac{T(I+1,J,K) - 2T(I,J,K) + T(I-1,J,K)}{[R(I) - R(I-1)]^2} \qquad (33)$$

Convection in the flow direction is

$$\rho C_p u \frac{\partial T}{\partial r} = q_c \qquad (34)$$

In difference form

$$q_c = RHOCP * \frac{VEL(I,J,K) + VEL(I-1,J,K)}{2} * \frac{T(I,J,K) - T(I-1,J,K)}{R(I) - R(I-1)} \qquad (35)$$

The CGS units of either term are [cal cm^{-3} sec^{-1}].

Thus, one can calculate each quantity, approximately, at any point.

Consider a 0.635 cm disk being filled under an applied pressure of 7500 psi for a melt entering at 202°C and cooling because of 30°C cavity walls.

At I = 11, J = 11 and t = 2.75 sec, in the hot melt region, we find that $q_d = -7.38 \times 10^{-5}$ and $q_c = 123.0 \times 10^{-5}$. Thus, radial conduction is negligible in the hot melt region.

When the rigid PVC in the vicinity of the cold wall cools below T_g, a new solid phase is formed and the boundary condition (25) changes. Heat from the melt is first conducted through this frozen layer and then out through the cold steel walls. More correct boundary conditions are

$$k \left.\frac{\partial T}{\partial x}\right|_{x = h_e/2} = \frac{K(\text{solid PVC})}{d(\text{solid PVC})} \left[T(r,h_e/2,t) - T(r,x,t)\right] \qquad (36)$$

and

$$K \left.\frac{\partial}{\partial x}\right|_{x = h/2} = L \left[T_o - T(r, h/2, t)\right]$$

A slight change in the results is obtained and since incorporation of the above feature for the "frozen skin" region requires lengthy programming additions, it was not included in the numerical solution of the energy equation. Finally, temperature dependence of thermal conductivity and heat capacity can be included in the solution.

RESULTS AND DISCUSSION

Rigid PVC melts were considered with Power Law constants of $n = 0.5$ and $m\ (202^{\circ}C) = 4 \times 10^{7}$ poises. The activation energy for flow was taken as 27.8 Kcal/g mole.[9] On Fig. 2 pressure of the non-isothermal as well as isothermal flow is plotted as a function of radius at various times of flow. For the non-isothermal case ($T_1 = 202^{\circ}C$ and $T_o = 30^{\circ}C$) where both VED and cooling are present, the pressure profile along the disk at a given instant shows considerable deviation from the idealized isothermal pressure profile. Initially, VED predominates and lowers the melt viscosity. This prevents the pressure at the disk entrance from reaching as high a level as it did when no VED was present. The net result is a more gradual pressure gradient. Then, because of the longer contact times with the cold walls, cooling becomes controlling. This increases the viscosity and PLEVEL rises above the value it had when cooling was neglected. The resulting steeper pressure gradient is mitigated only when the presence of frozen polymer near the front constricts the flowing melt and intensifies VED.

On Fig. 3 we see the effect of varying the applied pressure on the normalized flow rato (Q_T/Q_o) and front position (R/b) for an 0.3175 cm thick

disk with walls at 30°C. The initial polymer temperature is 202°C.

At 5000 psi the flow rate decline is gradual but with a steeper slope initially. The 7500 psi curve begins above, but then falls below the 5000 psi curve by not losing its steeper slope as quickly. At 11,600 psi the flow curve is again initially above but ultimately below both curves representing the lower pressures. The increase viscous heating of the flows at the higher pressures is responsible for their ability to maintain higher flow rates initially, because of the accompanying drop in viscosity. The hotter melt simply has a lower viscosity. However, when cooling begins to predominate, flow retardation is more intense because the non-isothermal situation is more extreme. Naturally, increasing the applied pressure advances the front more quickly.

In PVC whenever flow is accompanied by a high amount of VED, the problem of thermal degradation appears.[9] Since increasing the pressure has the effect of raising the average temperature through viscous heat generation, more degradation will be observed at higher pressures. The effects or degree of thermal degradation have not been introduced in the numerical solution.

On Fig. 4 one can see the effect of varying the plate separation on the normalized flow rate for a disk being filled with a PVC melt at 202°C under 5000 psi. The wall temperature is 30°C. As the mold cavity becomes thinner the flow rate falls off more rapidly. The narrower gap imposes a physical resistance to flow which can be seen in terms of the steeper pressure gradient and higher shear rate. More energy is absorbed as viscous heat generation. Therefore, thermal degradation of PVC may be a problem in thin cavities. Resistance to flow due to cooling is also playing a role in the diminishing flow rate.

On Fig. 5 one observes the effect of varying plate separation on the front position for the same conditions as the previous figure. As expected

after a given time interval the thinnest disk has the largest radius. Even with a relatively high flow rate sufficient material does not flow into the thicker disk in the same time interval to reach the same radius.

On Fig. 6 we observe the effect of varying the melt temperature T_1 on the normalized flow rate and the front position for a disk having 0.3175 cm plate separation which is being filled under a constant applied pressure of 7500 psi. When the wall is at 30°C, the flow rate of the coolest melt at 194°C falls off with the least rate, whereas the flow rates of the hotter melts at 202°C and 210°C ultimately show a more drastic decline as the difference between the initial melt temperature and the mold temperature increases. We notice that initially the hotter melts maintain a nearly constant flow rate for a length of time which increases with increasing melt temperature T_1. This is a VED effect; the heat generated at the high flow rates lowers the local viscosity near the entrance which allows the polymer to flow for a short time at nearly a constant rate. Then cooling from the 30°C walls becomes controlling and a drastic drop in flow rate occurs. In the case of the 194°C melt not enough heat is generated to make this effect apparent and only a gradual decrease in flow rate is evident. However, even here the VED is apparent when the initial portion of this curve is compared to an assumed isothermal situation (no VED and $T_0 = 202°C = T_1$). The greater amounts of VED generated by the hotter melts will increase the amount of thermal degradation in these non-isothermal flows.

As expected the hotter the melt the further the polymer front advances in a specified length of time. For example, at 0.5625 seconds the melt which entered at 210°C has filled 57.7% of the disk cavity as compared to 22.8% for that which entered at 194°C.

In view of the marked difference in the flow rate curves for the non-isothermal and isothermal curves for the 202°C melt, the fact that the front

positions do not differ markedly also, is somewhat surprising. Both cavities are 36.2% full after 0.5625 seconds. By visual inspection it appears that the area under the two corresponding Q vs t curves are about equal; it is this quantity (volume) that determines how much of the cavity has filled with melt. The implication here is that as long as estimating fill times is the primary concern the isothermal model is adequate. Simulations under a number of different conditions support this conclusion. An explanation and some comments regarding its reliability can be found in the discussion of Fig. 7.

Barrie[6] in his treatment did assume that the front position R was independent of the thermal environment. To account for non-isothermal effects he only changed h in the isothermal equations 4 and 5.

Since our work endorses this assumption and predicts that the difference in PLEVEL in the two cases is about 4 1/2% (see Fig. 8), Barrie's success in estimating PLEVEL based on empirically fitting a simple theoretical model is probably more than a happy coincidence.

Two sets of physical conditions are compared on Fig. 7. An isothermal fill, with both the polymer and cavity wall at 202°C, is contrasted with the same 0.635 cm thick disk being filled at the same pressure but with the wall at 30°C. The applied pressure is varied and the non-isothermal and isothermal flow processes are looked at again. Increasing the applied pressure shortens the time required to fill the cavity, irrespective of the thermal environment. At 11,600 psi, whether the wall is at 30°C or 202°C has no discernible effect on where the front is at a particular instant or the time it takes to fill the cavity. However, at the lower pressures the simulation shows that the non-isothermal filling actually occurs sooner, although initially no effect on the position of the polymer front is evident. One explanation for this effect is that VED is more pronounced. Thus, increasing the applied pressure

makes the injection cycle more insensitive to temperature variations.

In Figs. 8 and 9 a comparison of an isothermal ($T_1 = 202^oC = T_o$) and a non-isothermal ($T_1 = 202^oC$; $T_o = 30^oC$) cavity filling process is made in terms of the pressure developed at the disk entrance, PLEVEL. Results are illustrated for constant applied pressures of 5000, 7500 and 11,600 psi. The plate separation is 0.635 cm. In the non-isothermal sitations PLEVEL gradually increases as material flows into the disk cavity and reaches about 14.5% of the applied pressure (PRES) just prior to fill. The isothermal cases are characterized by PLEVEL initially increasing more rapidly but only reaching 11.1% of PRES just prior to fill.

The crossover of the non-isothermal and isothermal curves was also observed with the flow rate curves (see Fig. 3). The fact that they occur at almost the same time, strongly suggests a cause-effect relationship between PLEVEL and flow rate, but it could also be fortuitous. Initially the VED in the non-isothermal filling lowers the viscosity and prevents PLEVEL from building up. As cooling becomes controlling PLEVEL rises sharply followed by a gradual increase as the cooling rate diminishes. The absence of VED in the isothermal case allows the melt to experience cooling immediately; PLEVEL is proportional to the increasing viscosity. As the pressure is increased, the higher VED generated makes this difference in behavior more obvious.

Illustrated in Fig. 10 for comparison are the velocity and temperature profiles of an isothermal and non-isothermal moving front the instant just before fill occurs in a 0.635 cm cavity under an applied pressure of 7500 psi. The presence of a cold (30°C) wall drastically decreases the velocity gradients near it. Thus, high velocity gradients with VED predominating are observed. These effects are responsible for the "nipple-like shape" of the non-isothermal velocity profile. The almost stationary polymer near the cold wall is what is referred to as the "frozen polymer wall" which reduces the available

cross-section, thereby, raising the shear rate and increasing the VED in the moving polymer. The non-isothermal temperature profile can also be described as a flattened parabola with the higher temperatures near the centerline. The fact that it lies entirely below the isothermal temperature profile is peculiar to the case at hand. Were the initial melt temperature greater or the cavity more narrow or the applied pressure higher, it is likely that some of the center portion would lie above the horizontal line which represents the isothermal temperature profile.

On Fig. 11 we see the shear rate profiles corresponding to the velocity profiles of Fig. 10. For isothermal flow the shear rate increases from zero at the centerline to a maximum at the wall. This maximum lies between the centerline and the wall in the isothermal case. The cooling effect of the cold wall renders the polymer in its vicinity nearly immobile, assuring low shear rates in that region. Too far from the wall to experience cooling, the gradually rising shear rate is augmented by the generation of viscous heat which lowers the viscosity. The sharp rise is followed by an even sharper drop when the walls are near enough for cooling to become controlling.

On Fig. 12 the effects of the computational times increment, Δt , on the average melt temperature and the position of the front are shown under conditions that result in rapid filling. The front position is independent of the Δt employed, but the average melt temperature depends on it strongly. For reasons of computer storage it has not always been possible to keep Δt properly small and still carry the calculation far enough to fill cavities. Fortunately, the cooling effect is so overwhelming as the melt advances into the cavity that the average front temperatures based on different Δt's approach each other near the outer radius of the disk. Nevertheless, if one wants to calculate the extent of resin degradation, due to increased temperatures, then very small increments of time, about 2×10^{-3} sec, would have to

be used in the numerical solution.

On Fig. 13 the average melt temperature as the filling process proceeds is plotted for two pressures and two wall temperatures at $\Delta t = 0.05$ sec. It is observed that the wall temperature does not have nearly as large an effect on the temperature as that of pressure. Thus, if degradation of the PVC resin is a problem lowering the pressure and not the mold temperature would be of help.

In practice the ambient temperature of the mold surface varies considerably. The thermal environment of the first few pieces is entirely different than that of subsequent cycles, since the room temperature varies and cold mold surface heats up. Nonetheless, it is not usual to find elaborate cooling equipment because no significant improvement in quality or cycle time is observed. This is as predicted by the simulation.

In Fig. 14 one can observe the effect of VED in the tube on flow rate and front position. Q_o is 32.4 cc/sec for both cases. The initial polymer temperature is 202°C, but when VED in the tube is considered, the melt initially enters the disk at 222.41°C[9,19]. The flow rate declines more rapidly than when an isothermal tube was assumed and is accompanied by a slower rate of filling. The primary reasons for the slow filling are that flow in the disk is determined by ZLEVEL, which the hotter melt prevents from building up, and that the applied pressure needed to establish Q_o is 2000 psi less if the polymer heats up to 222.41°C during its travel through the tube, so that there is less applied to begin with. It is also true that the velocity gradients imposed initially on the two flows will be more severe for the hotter melt near the wall.

CONCLUSIONS

The following conclusions can be reached from the numerical solution of the coupled momentum and energy balance equations which describe the mold filling operation of rigid PVC melt in a disk cavity.

In the range of process variables that we investigated it was found that the "fill times" of non-isothermal and isothermal melt flow were almost identical, despite the fact that they differed in all other respects. Although we have no clear explanations for this result, its practical implications are clear. There is no computational need of including the energy equation in the solution of the problem, if obtaining mold filling times is the only information sought. Any further work on this problem should investigate a larger range of processing variables and material parameters to determine whether isothermal and non-isothermal fill times are nearly equal in general. The above result also justifies the isothermal assumption of Barrie who in his treatment attempts to predict the macroscopic aspects of the mold process. The agreement between his largely empirical treatment and experimental results can now be understood. Furthermore, because he has looked at a different polymer resin, an ethylene-propylene copolymer we suspect that our findings on the similarity between isothermal and non-isothermal fill are more general.

The similarity of Figs. 3 and 6 establishes the existence of a pressure-melt temperature equivalence. Raising the source pressure has the same effect on flow rate and front position as increasing the initial melt temperature; this similarity can be extended to the temperature profile.

The full non-isothermal non-Newtonian melt description of the problem is needed to obtain detailed information on the process, such as information leading to the establishment of the extent of resin viscous heating and degradation, distribution of the residual or "frozen" strains and distribution

of the residual pressure along the radius of the mold cavity. This is precisely the information that is needed for large part molding and that our solutions provides approximately. The results are approximate and correct only in a semi-quantitative sense because of the limitations that the digital computer system of Stevens Institute imposed on the solution. Specifically, the computational difficulties can be stated as follows: The problem is three-dimensional. In the difference form of the transport equation a time increment Δt has to be used. This should be kept appropriately small so that not only convergence to the solution of the differential equation is achieved, but from a more practical point of view, no temperature instabilities are obtained numerically. Whereas, it was always possible to keep Δt small enough to achieve the latter, the system's maximum core capacity of 27K imposed a lower limit on Δt if the outer radius of the mold cavity to be filled satisfied the condition that $b \gg h$, the basis of the lubrication approximation. The execution time for Case IV simulation when 27K was utilized was about 28 minutes. Because of these system limitations there is no guarantee that convergence to the differential solution was achieved. Therefore, the values obtained for $T(r,x,t)$, $u(r,x,t)$, etc. may not be quantitatively correct, which is why we report the detailed results in a semi-quantitative fashion.

The simulation affords a means of looking at both the average temperature and the detailed temperature profile at a particular flow radius. Since a significant amount of frozen polymer may be present even when the average temperature is well above T_g or T_m, generalizations based on average temperature may be misleading. A detailed examination of $T(r,x,t)$ on the other hand does provide insight into several phenomena with which the practical molder must contend. For example, the build up of a frozen polymer skin near

the wall as the hot melt flows into the cavity, and the creation of intense VED at the core which may initiate or intensify thermal degradation in a resin such as PVC. By providing the temperature and pressure profiles at the instant of fill, realistic initial conditions are now available for solving the related problems of how the pressure in the disk increases during the packing stage and how the molded part cools under pressure. From these solutions final frozen strains in the material and the residual pressure may be obtained. Both are intimately related to the quality of the molded part.

For non-isothermal flows which ignored VED in the tube entrance, the pressure at the disk entrance was 14.5% of the source pressure at the instant of fill. Under these conditions the gate and runners have a profound effect on lowering the efficiency of the cycle by dissipating the bulk of the applied pressure before it has a chance to advance the melt into the cavity. If this were available at the disk entrance there is no question that the mold would fill much faster. Melt which is heated by VED during its travel through the tube will be delivered at the disk entrance either at the same flow rate under a lower source pressure, or at a higher flow rate under the same pressure. The development of PLEVEL will be hindered by the lower viscosity of the melt exiting from the tube and it should not reach 14.5% at the fill instant in either case. Consequently, a low PLEVEL and a lower source pressure might result in longer fill times because of the increased flow rate. This will generate more intense viscous heating throughout the cavity as it fills. Based on these observations we conclude that the gate and runners are the most important factors to be considered in mold design. Ignoring their effect in future studies may be the most important reason for failing to predict actual filling behavior.

It is not surprising, in view of this study, why the fancy design of the runner system has been responsible for successfully filling large molds. By

carefully designing the corners in runners and using hot multigated runner manifolds, the adverse pressure and viscous energy dissipation effects of the entrance can be lessended.

Experiments to quantitatively support or refute the predicted flow behavior would be the most valuable supplement to this work. Furthermore, the work should be completed for rigid PVC and then continued with other materials. The fact that four separate computer programs are available to solve the disk flow problem provides a wide range of many materials and modifications. For rigid PVC degradation kinetics mechanism should definitely be incorporated in the simulation. In thermosetting resins too, the increase in viscosity due to cross-linking may be of interest. The dependence of density, specific heat, thermal conductivity and activation energy for flow on temperature and pressure will also have to be considered.

BIBLIOGRAPHY

1. C. W. Deelyey and J. F. Terenzi, Mod. Plast., 42, No. 12, 111 (1965).
2. F. C. Karas, Mod. Plast., 41, No. 1, 140 (1963).
3. D. H. Harry and R. G. Parrott, Pol. Eng'g. Sci., 10, No. 4, 209 (1970).
4. S. Kenig and M. R. Kamal, SPE Journal, 26, 50 (1970).
5. J. R. A. Pearson, "Mechanical Principles of Polymer Melt Processing," Pergamon Press, Oxford (1966).
6. I. T. Barrie, Plastics & Polymers, 38, 47 (1970).
7. F. N. Cogswell and P. Lamb, "Material Properties Relevant to Melt Processing" (to be published in Plastics & Polymers).
8. H. Fishenden and O. A. Saunders, "An Introduction to Heat Transfer," Clarendon Press, Oxford (1950).
9. R. A. Morrette and C. G. Gogos, Pol. Eng'g Sci., 8, No. 4, 272 (1968).
10. R. Cintron-Cordero, Stevens Institute of Technology, private communication.

11. R. B. Bird, W. E. Stewart, E. N. Lightfoot, "Transport Phenomena", John Wiley & Sons, Inc., New York (1960).

12. R. D. Hartree, "Numerical Analysis" Oxford University Press (1958).

13. L. M. Kells, "Calculus", Prentice-Hall, Inc., New Jersey (1949).

14. F. B. Hildebrand, "Advanced Calculus for Applications", Prentice-Hall, Inc., New Jersey (1962).

15. P. Laasonen, J. Assoc. Computer Mach., 5, 32 (1958).

16. J. Crank and P. Nicholson, Proc. Cambridge Phil. Soc., 43, 50 (1947).

17. L. Lapidus, "Digital Computation for Chemical Engineers", McGraw-Hill Book Company, New York (1962).

18. G. H. Bruce, D. W. Peaceman, H. H. Rachford and D. Rice, Trans. AIME, 198, 79 (1953).

19. N. Curto, Owens-Illinois Technical Center, Toledo, Ohio, private communication.

20. T. W. Huseby, Bell Telephone Laboratories, Murray Hill, New Jersey private communication.

21. R. J. Lugt, Naval Ship Research and Development Center, Washington, D. C., private communication.

22. A. J. Chapman, "Heat Transfer", John Wiley & Sons, Inc., New York (1967).

23. C. L. Mantell, "Engineering Materials Handbook", McGraw-Hill Book Company, New York (1958).

APPENDIX

Rigid PVC Properties Used

Power law index $n = .5$

Consistency index $m = 4.0 \times 10^5$ poise 202°C

Pre-exponential factor for the temperature dependence of viscosity $A = 6.46 \times 10^{-8}$,

Activation energy for flow $\Delta E = 27.8$ kcal/g mole

Density (melt) $\rho = 1.3$ gm/cc

Heat capacity $C_p = 0.43$ cal/g°K

Thermal conductivity $k = 2.3 \times 10^{-4}$ cal/g-sec°K

Temperature below which flow can be ignored $T_h = 150°C$ (not a material property)

ACKNOWLEDGEMENTS

The work was supported by the Office of Naval Research - Project THEMIS grant. Mr. Berger, while a graduate student, received fellowships from the National Science Foundation, the R. C. Stanley Foundation, the Plastics Institute of America and the National Aeronautics and Space Administration. The help of the above-mentioned agencies is greatly appreciated.

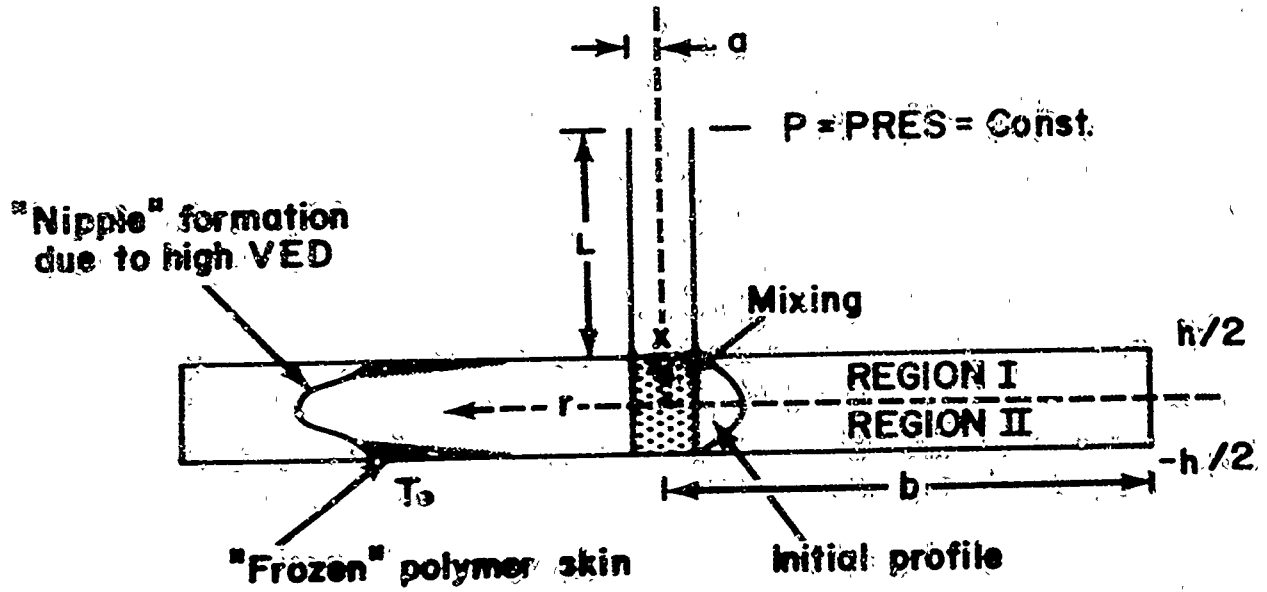

FIG. 1 THE DISK-SHAPED MOLD CAVITY

FIG. 2

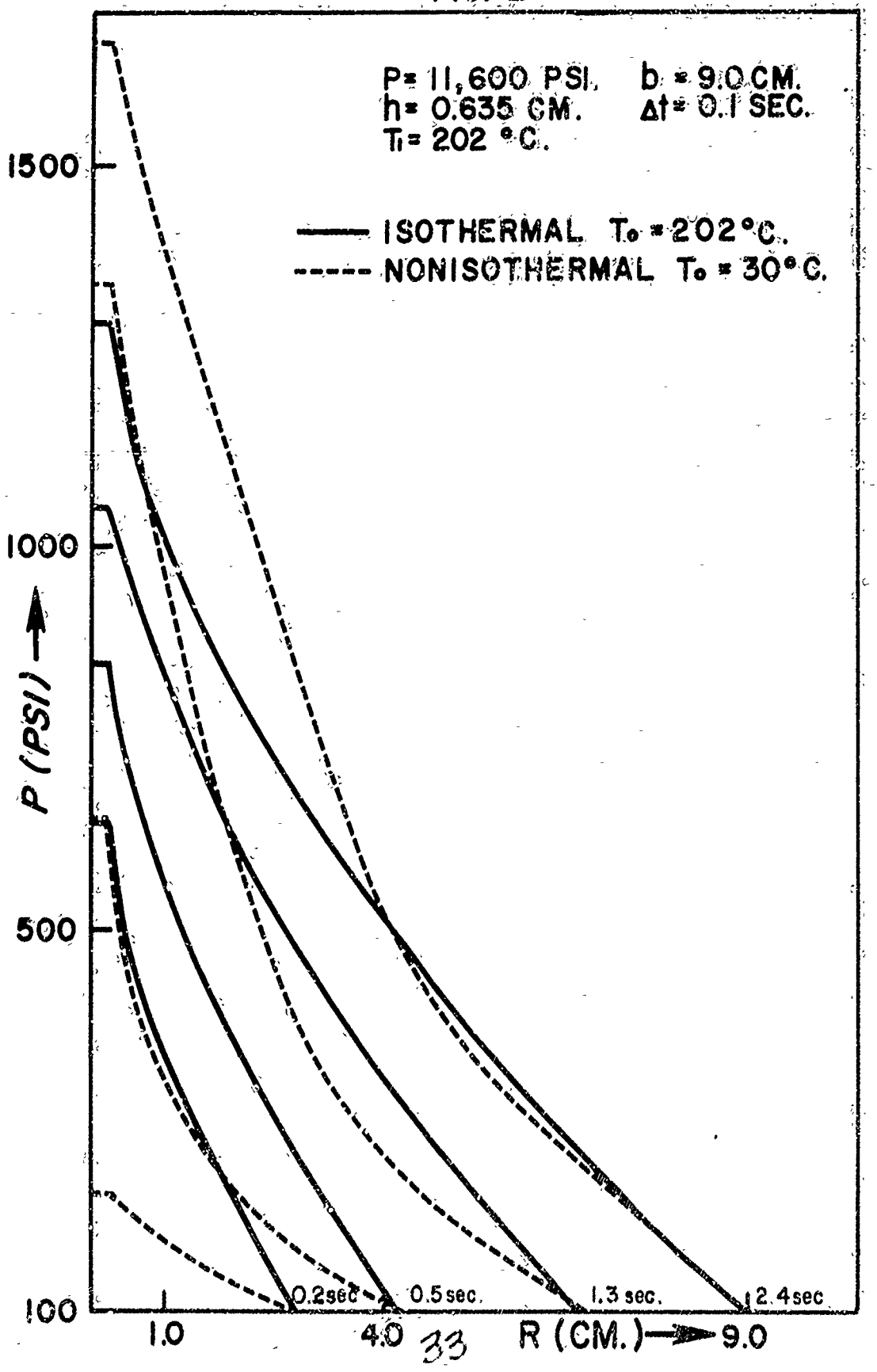
P= 11,600 PSI.
h= 0.635 CM.
Ti= 202 °C.
b = 9.0 CM.
Δt = 0.1 SEC.
ISOTHERMAL To = 202°C.
NONISOTHERMAL To = 30°C.
1500
1000
500
100
P (PSI)
0.2sec
0.5sec
1.3 sec.
2.4sec
1.0
4.0
R (CM.)
9.0

FIG. 3

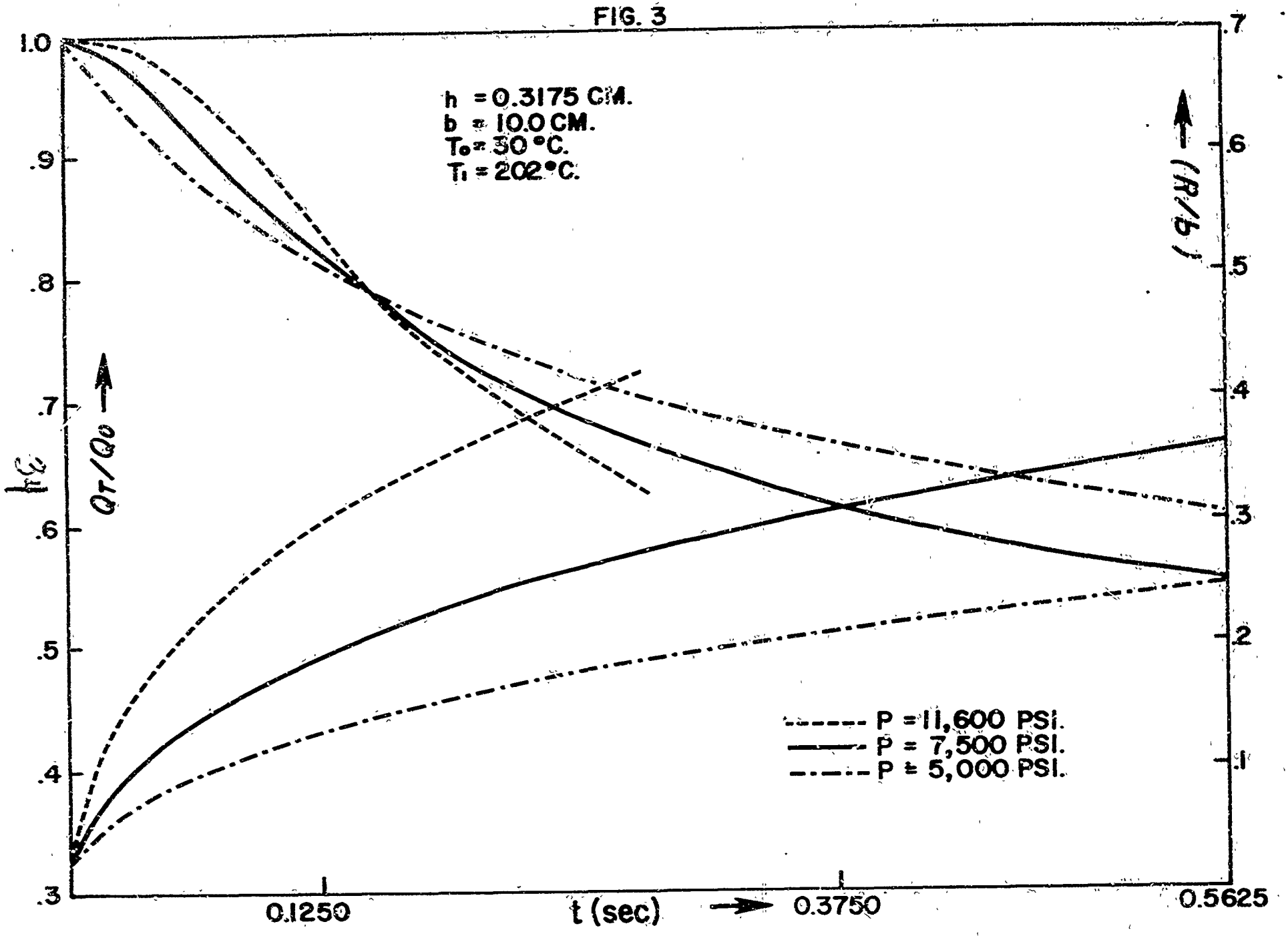
h = 0.3175 CM.
b = 10.0 CM.
To = 30 °C.
Ti = 202 °C.
QT/Qo
(R/b)
t (sec)
0.1250
0.3750
0.5625
P = 11,600 PSI.
P = 7,500 PSI.
P = 5,000 PSI.
1.0
.9
.8
.7
.6
.5
.4
.3
.7
.6
.5
.4
.3
.2
.1

FIG. 4

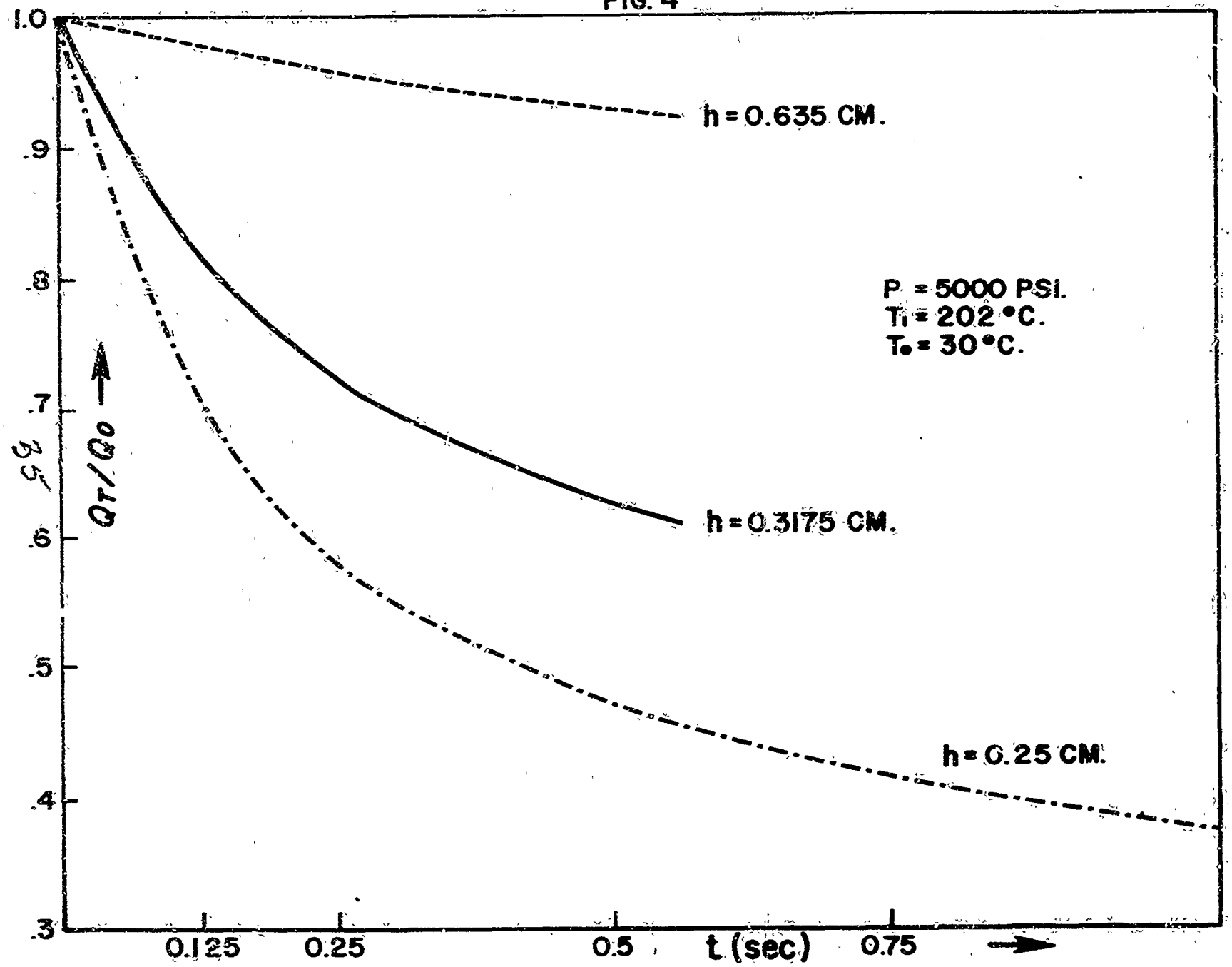
1.0
.9
.8
.7
.6
.5
.4
.3
Q_T/Q_o
h = 0.635 CM.
h = 0.3175 CM.
h = 0.25 CM.
P = 5000 PSI.
T_i = 202 °C.
T_o = 30 °C.
0.125
0.25
0.5
t (sec)
0.75

FIG. 5

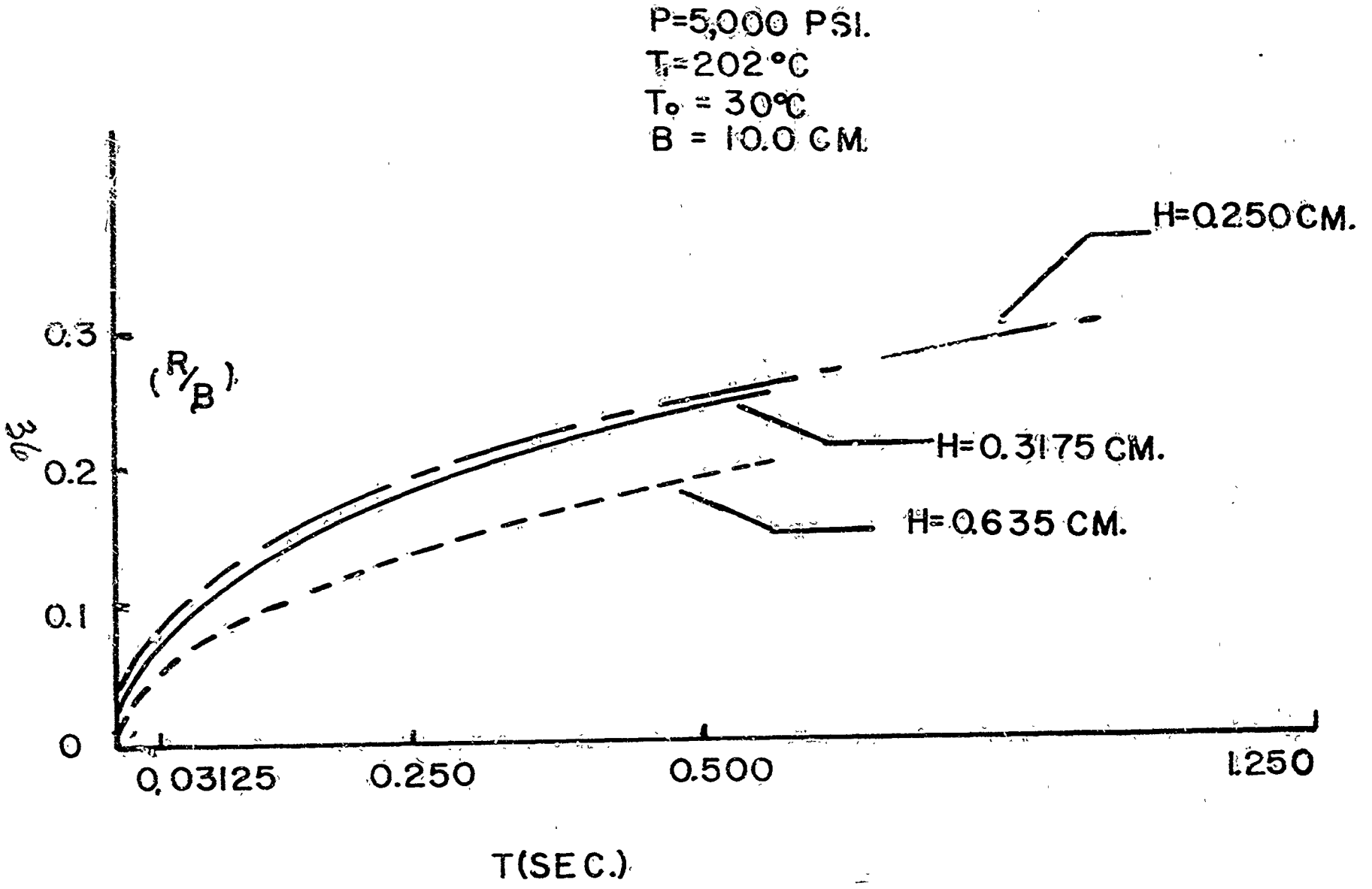
P=5,000 PSI.
T=202°C
To = 30°C
B = 10.0 CM.
H=0.250CM.
H=0.3175 CM.
H=0.635 CM.
(R/B)
0.3
0.2
0.1
0
0.03125
0.250
0.500
1.250
T(SEC.)

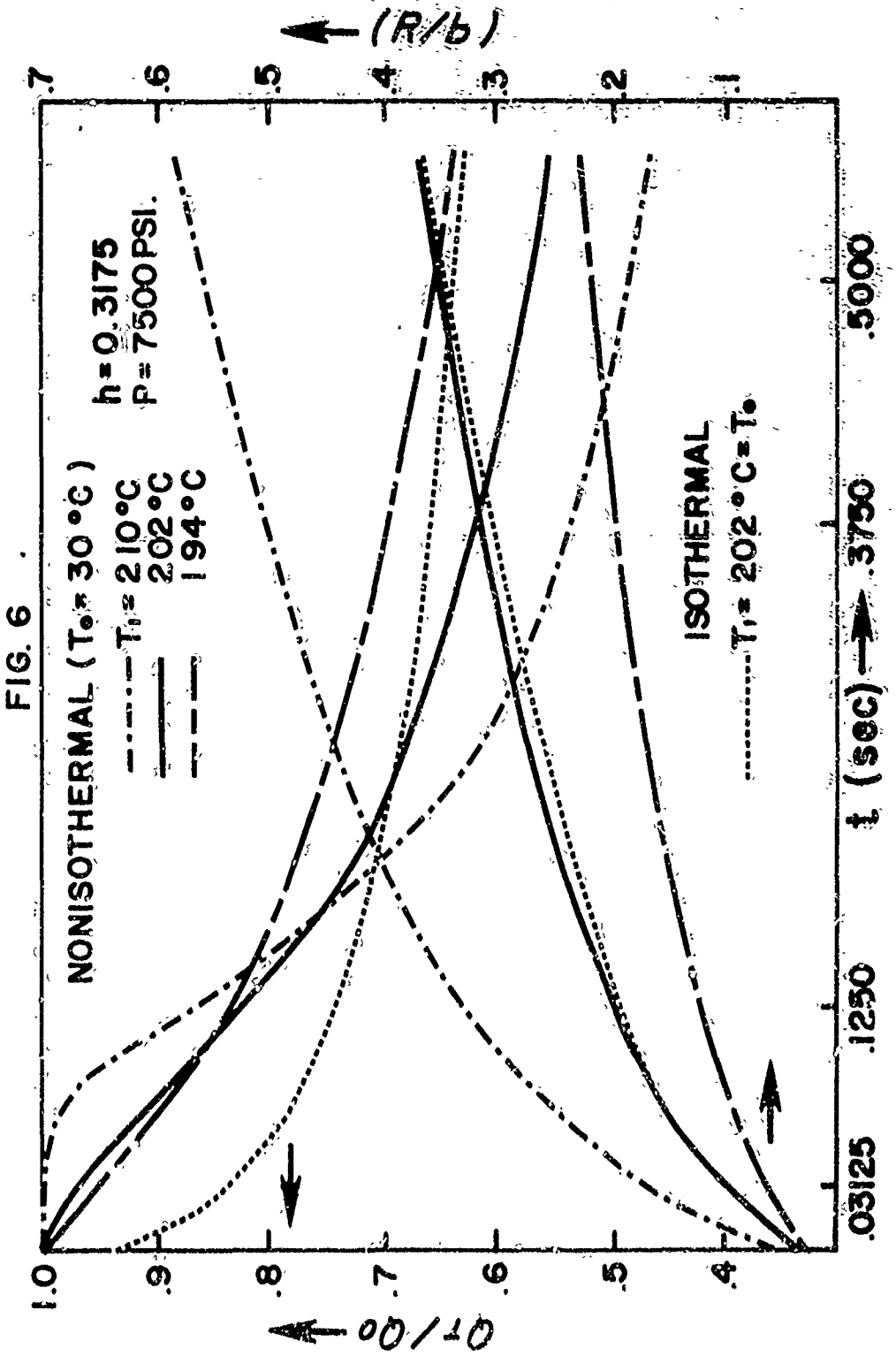
(R/b)
.7
.6
.5
.4
.3
.2
.1
h=0.3175
P=7500PSI.
NONISOTHERMAL (T₀= 30 °C)
T₁= 210°C
202°C
194°C
ISOTHERMAL
T₁= 202 °C = T₀
t (sec)
.03125
.1250
.3750
.5000
1.0
.9
.8
.7
.6
.5
.4
σθ/σ0

FIG. 6

FIG. 7

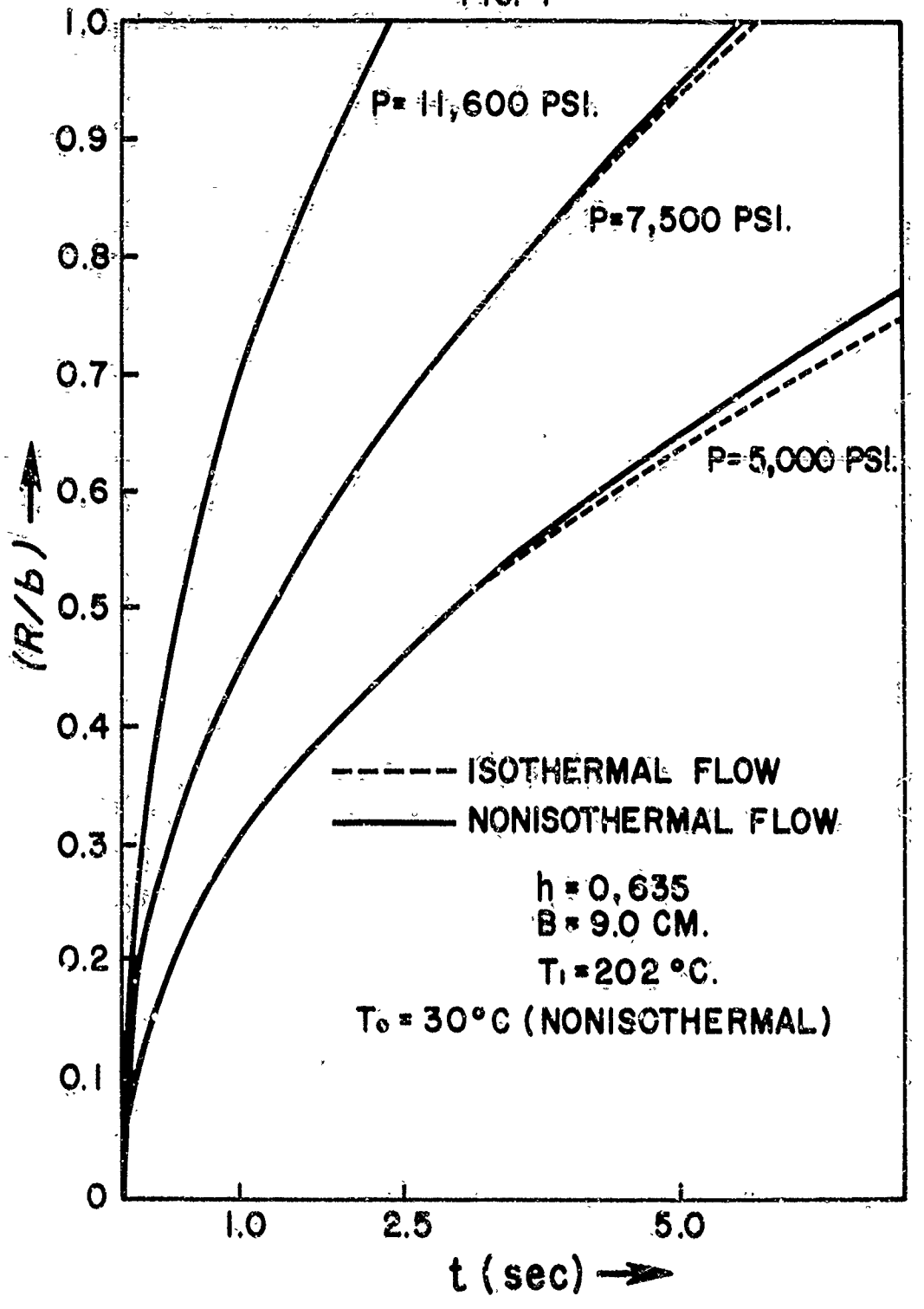
1.0
0.9
0.8
0.7
0.6
0.5
0.4
0.3
0.2
0.1
0
(R/b) →
P= 11,600 PSI.
P=7,500 PSI.
P= 5,000 PSI.
ISOTHERMAL FLOW
NONISOTHERMAL FLOW
h = 0,635
B = 9.0 CM.
T₁ = 202 °C.
T₀ = 30°C (NONISOTHERMAL)
1.0
2.5
5.0
t (sec) →

FIG. 8

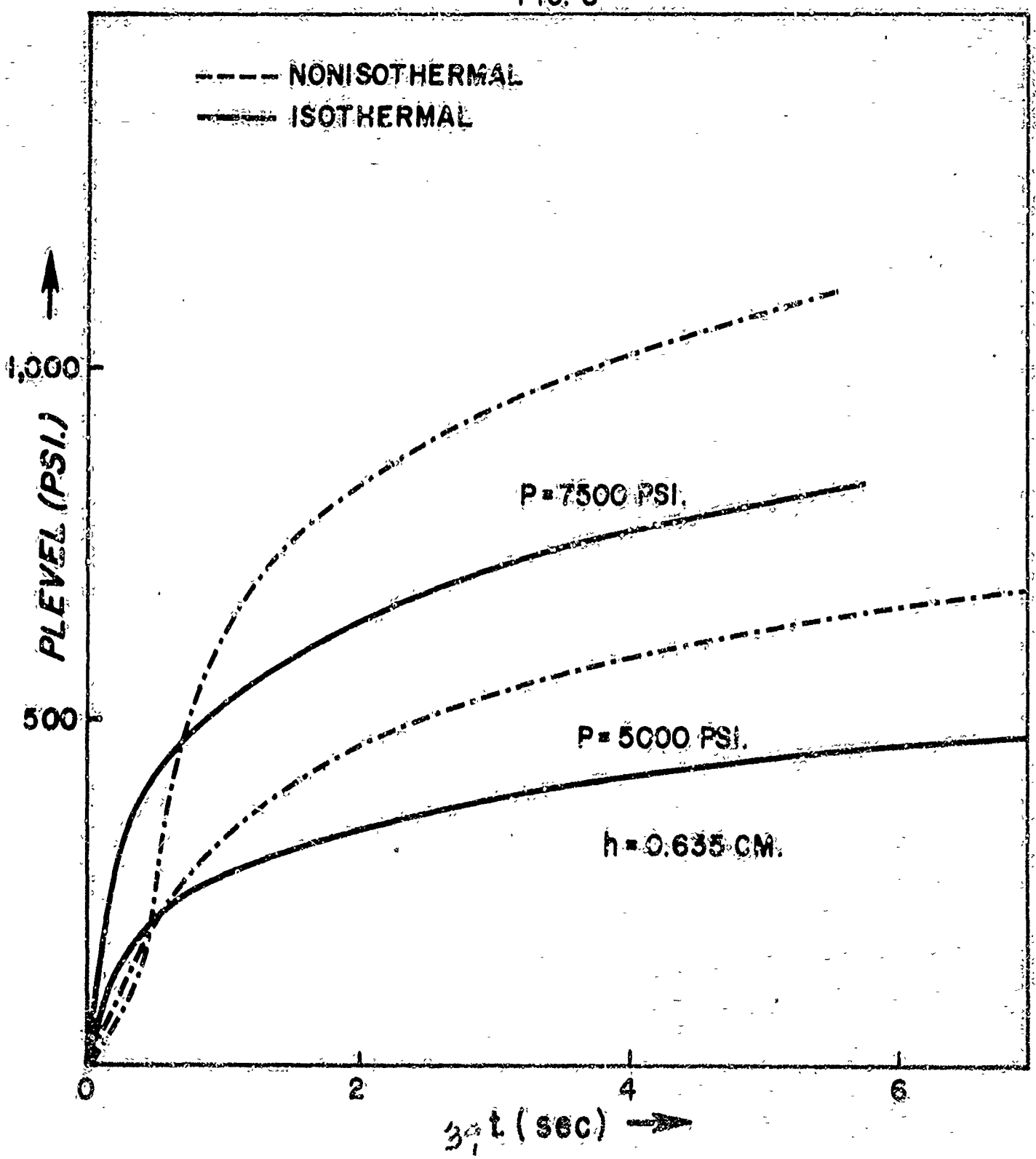
NONISOTHERMAL
ISOTHERMAL
1,000
500
PLEVEL (PSI.)
P = 7500 PSI.
P = 5000 PSI.
h = 0.635 CM.
0
2
4
6
t (sec)

FIG. 9

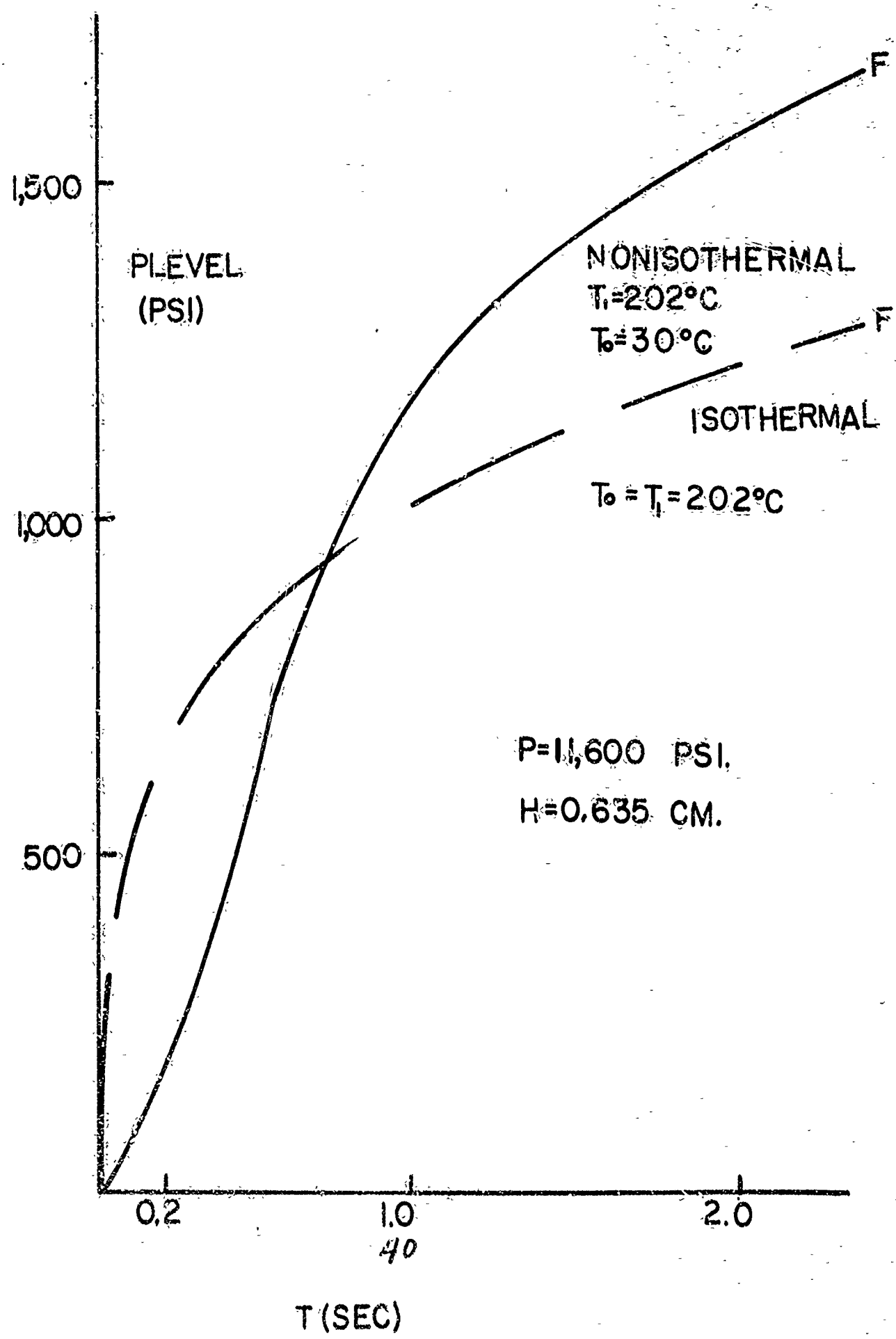
1,500
1,000
500
PLEVEL
(PSI)
F
NONISOTHERMAL
T₁=202°C
T₀=30°C
F
ISOTHERMAL
T₀ = T₁ = 202°C
P=11,600 PSI.
H=0.635 CM.
0.2
1.0
2.0
40
T (SEC)

FIG. 10

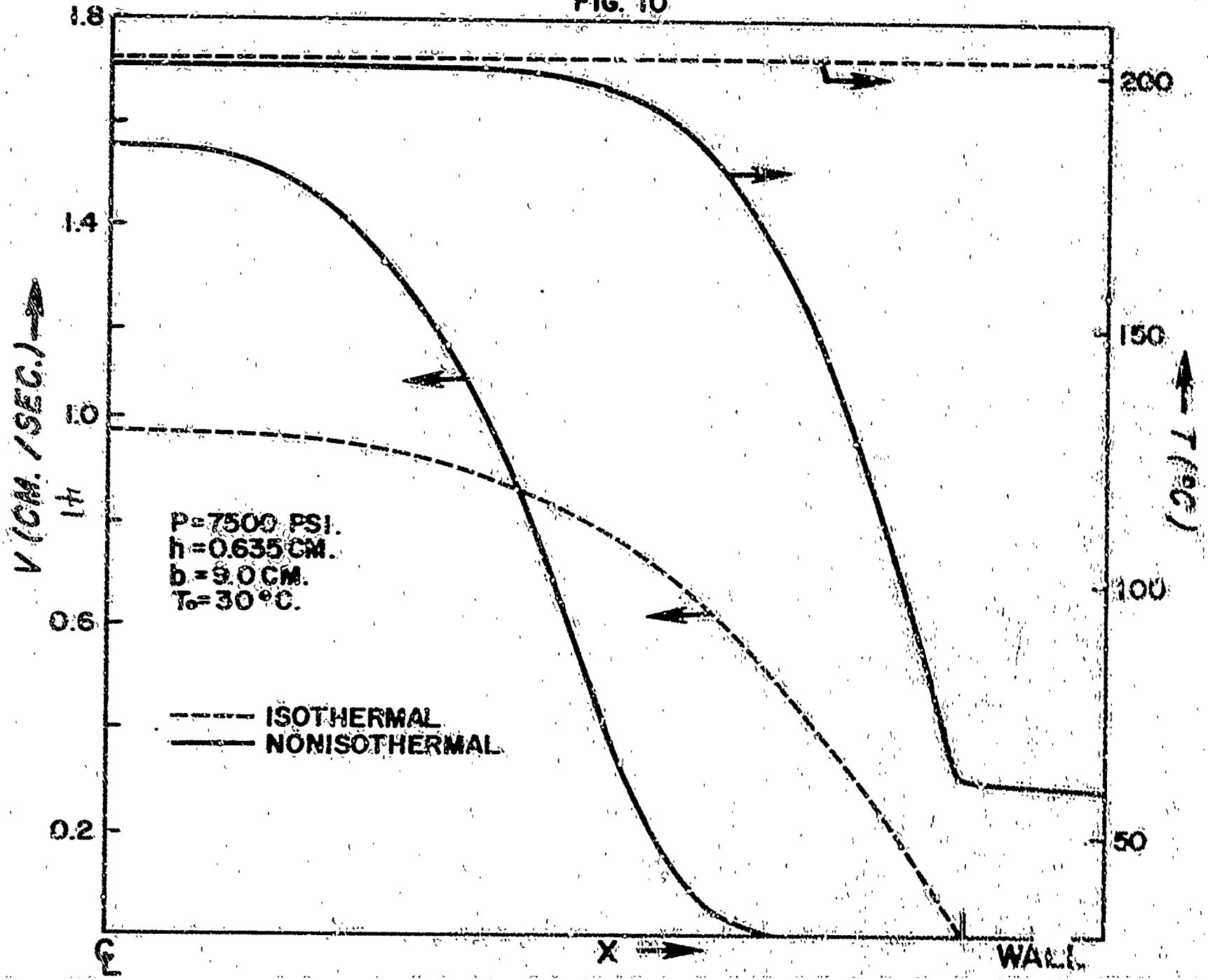
1.8
1.4
1.0
0.6
0.2
V (CM. / SEC.)
200
150
100
50
T (°C)
P=7500 PSI.
h=0.635 CM.
b=9.0 CM.
T₀=30 °C.
ISOTHERMAL
NONISOTHERMAL
X
WALL

FIG. 11

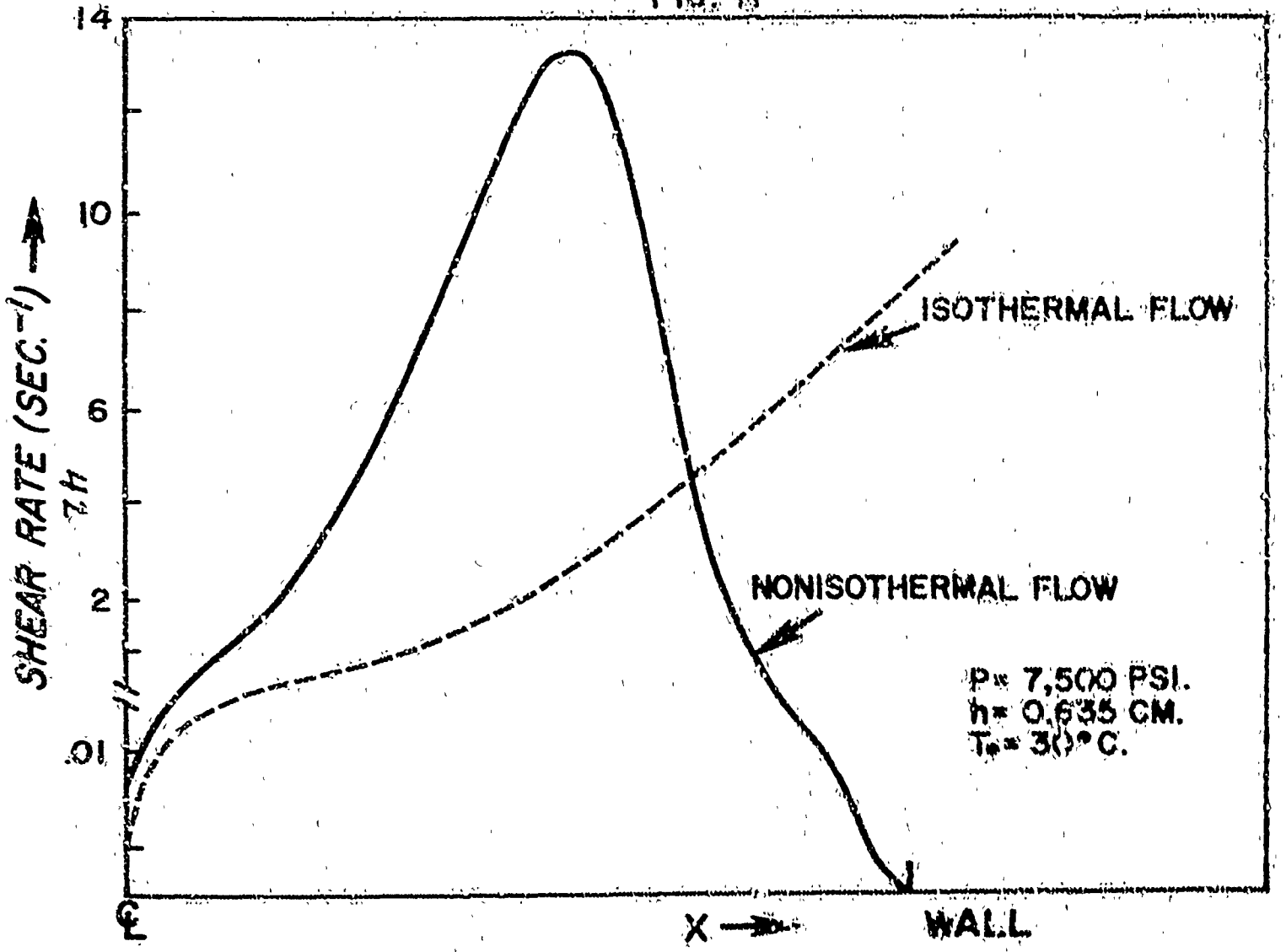
14
10
6
2
.01
SHEAR RATE (SEC.$^{-1}$) →
$\dot{\gamma}_h$
ISOTHERMAL FLOW
NONISOTHERMAL FLOW
P= 7,500 PSI.
h= 0.635 CM.
T_o= 30° C.
X →
WALL

FIG. 12

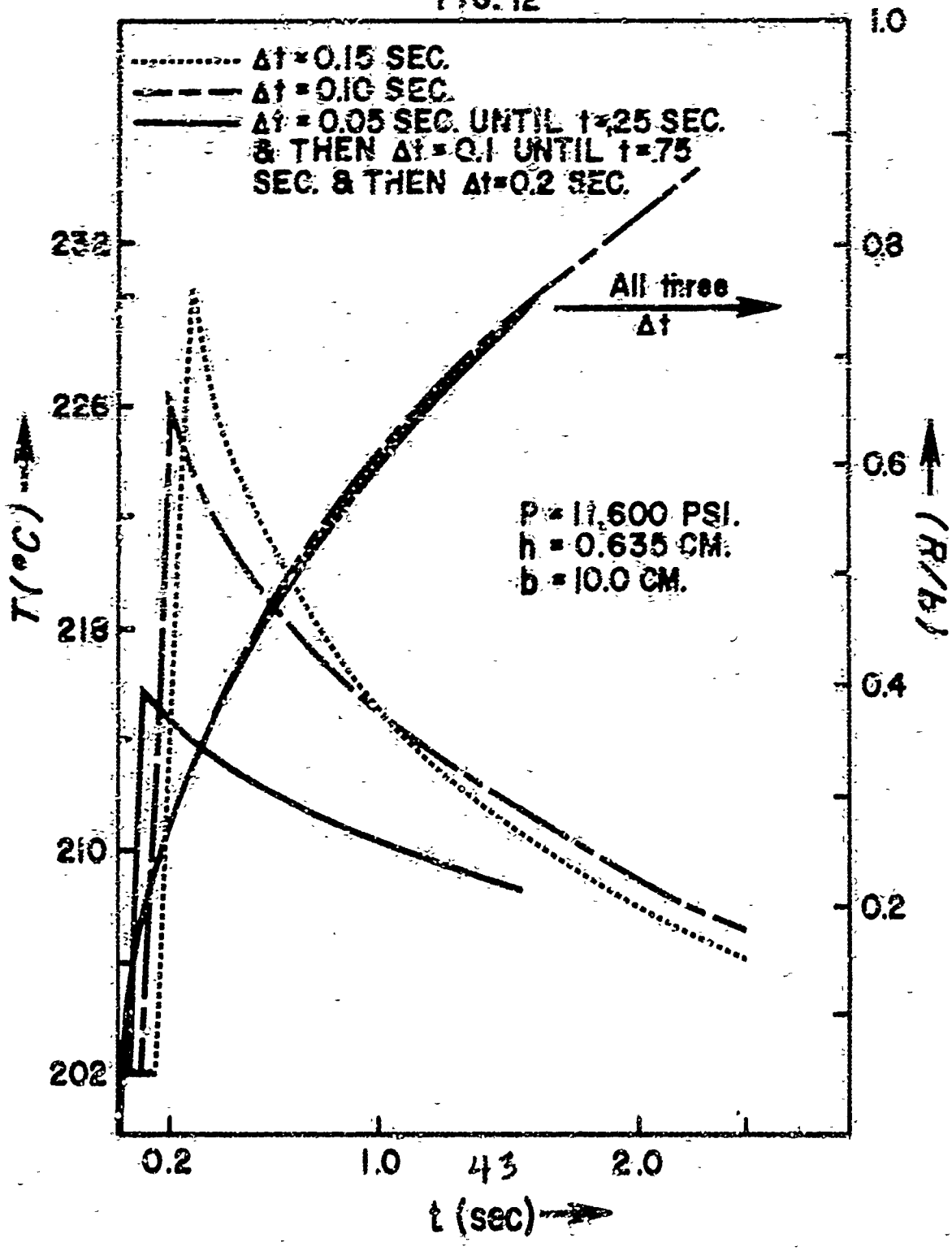
Δt = 0.15 SEC.
Δt = 0.10 SEC.
Δt = 0.05 SEC. UNTIL t = 1.25 SEC. & THEN Δt = 0.1 UNTIL t = 1.75 SEC. & THEN Δt = 0.2 SEC.
All three Δt
P = 11,600 PSI.
h = 0.635 CM.
b = 10.0 CM.
T (°C)
232
226
218
210
202
R/R₀
1.0
0.8
0.6
0.4
0.2
0.2
1.0
2.0
t (sec)

FIG. 13

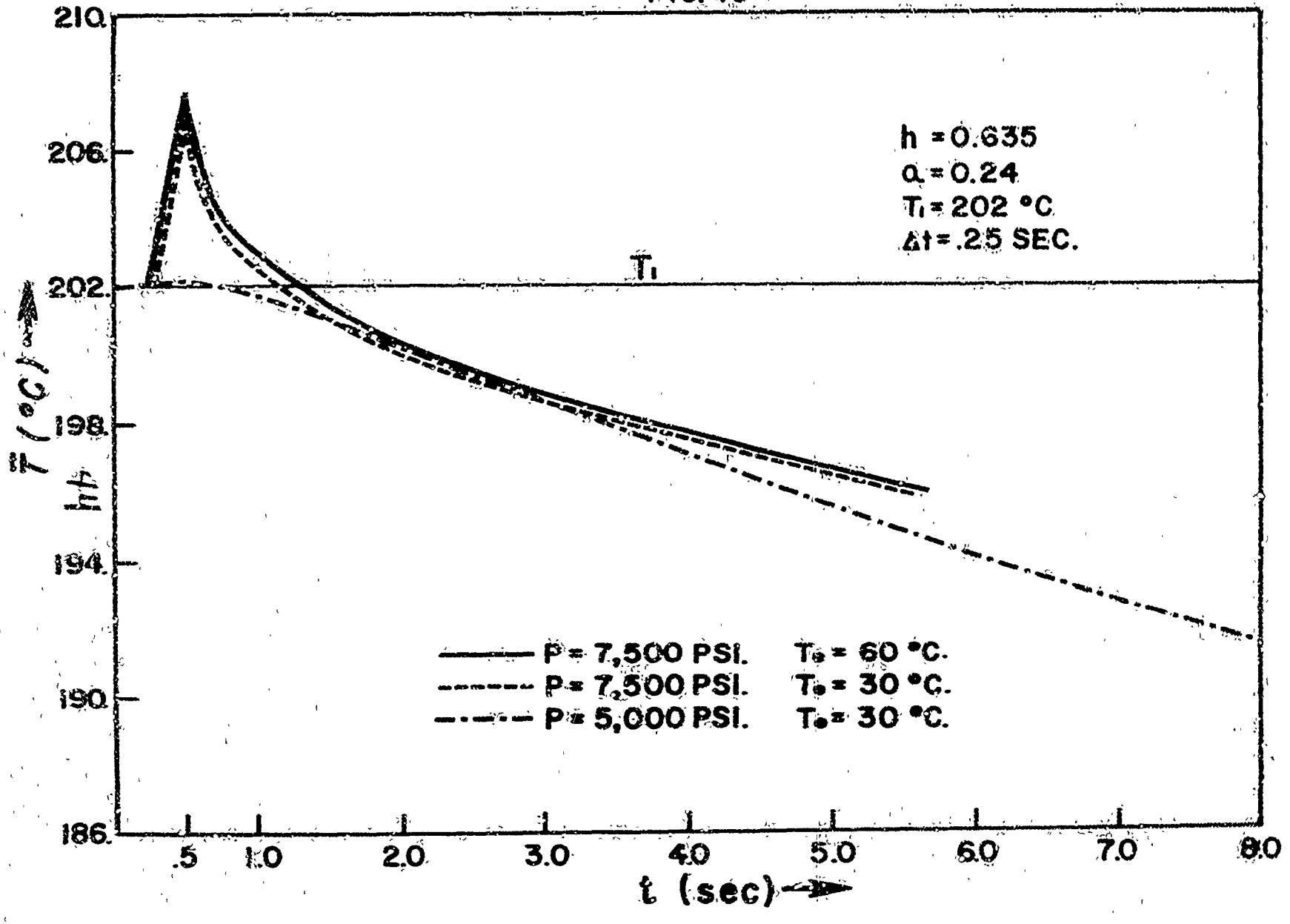
210
206
202
198
194
190
186
T (°C)
h = 0.635
a = 0.24
T₁ = 202 °C
Δt = .25 SEC.
T₁
P = 7,500 PSI. T₀ = 60 °C.
P = 7,500 PSI. T₀ = 30 °C.
P = 5,000 PSI. T₀ = 30 °C.
.5
1.0
2.0
3.0
4.0
5.0
6.0
7.0
8.0
t (sec)

FIG. 14

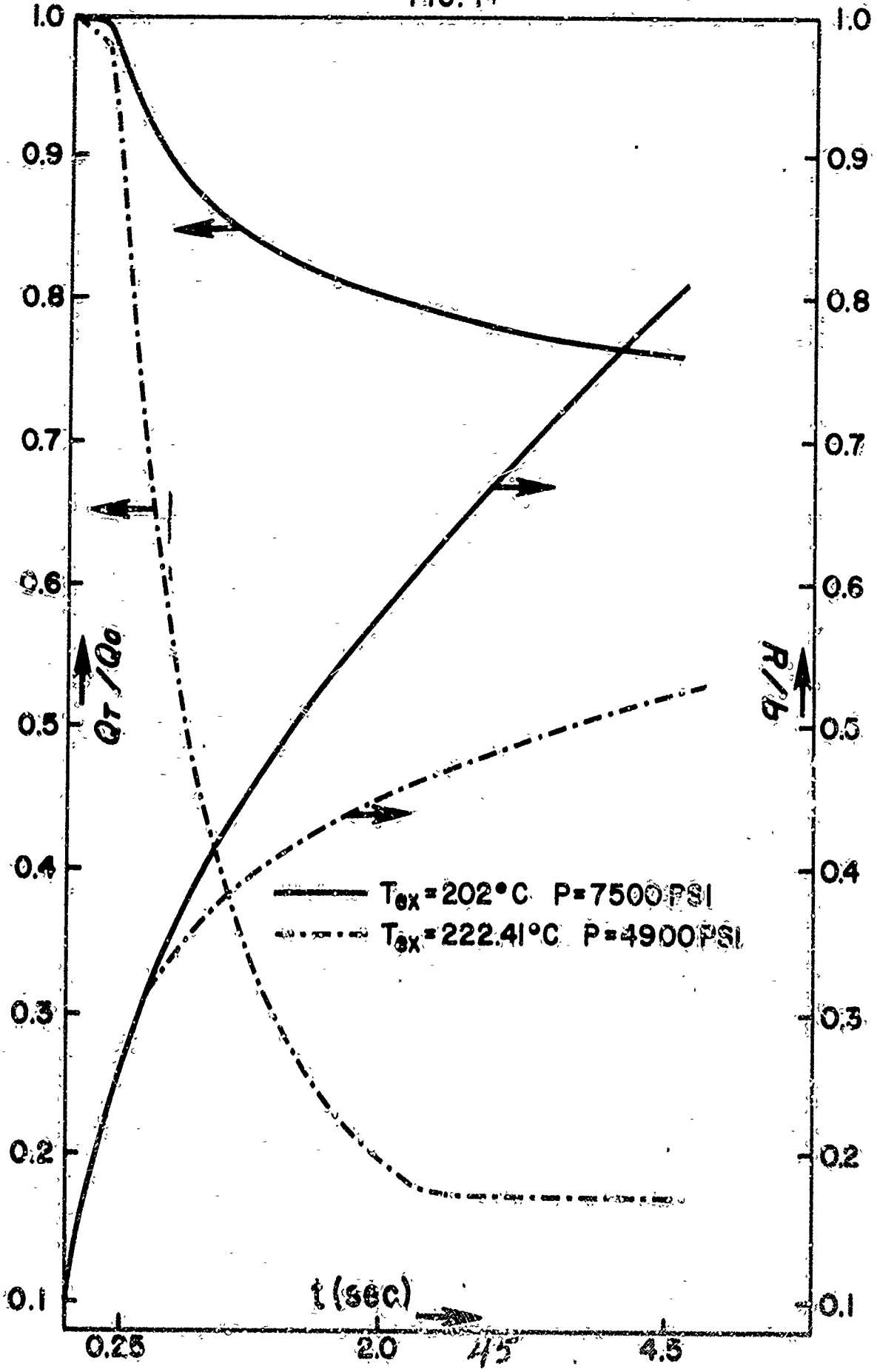
1.0
0.9
0.8
0.7
0.6
0.5
0.4
0.3
0.2
0.1
Qt/Qo
Q/Q
T_ex = 202°C P = 7500 PSI
T_ex = 222.41°C P = 4900 PSI
t (sec)
0.25
2.0
4.5